TRENDS IN COMPUTATIONAL STRUCTURAL MECHANICS
W.A. Wall, K.-U. Bletzinger and K. Schweizerhof (Eds.)

INTERFACING NONMATCHING FEM MESHES: THE ZERO MOMENT RULE

K. C. Park* **, Carlos A. Felippa and Gert Rebel**
Department of Aerospace Engineering Sciences
and Center for Aerospace Structures
University of Colorado, Boulder, CO 80309-0429, USA
e-mail: kcpark@titan.colorado.edu
web page: http://caswww.colorado.edu

Abstract. This is a tutorial paper that outlines, through a benchmark example, an effective method for coupling nonmatched finite element meshes. Coupling is done through a displacement *frame* interposed between the interface meshes. That frame is treated with a FEM discretization and "glued" to the meshes through localized Lagrange multipliers collocated at mesh-interface nodes. The approach can be used to couple meshes of arbitrary geometry, discretization type (e.g., FEM and BEM) and even meshes of different physics (e.g., structure and fluids). The example, however, focuses on a simplified 2D case that can be explained within space constraints. The requirement for preservation of constant stress states leads to an easily visualized condition, called the zero-moment rule or ZMR, that can be used to locate frame nodes on frame geometry. The ZMR provides all possible consistent frame-node configurations. Generalizations of the 2D ZMR rule to 3D problems involve partitioning of the frame and are not reported here. Thus the ZMR is necessary but not sufficient. The constant stress consistency condition may be interpreted, according to the reader's taste, as either an interface patch test, a vanishing of the first variation of the interface potential under admissible kinematic modes, or a requirement for energy conservation across the interface.

Key words: Finite element methods, nonmatching meshes, interface frame, localized Lagrange multipliers, constant stress consistency, interface potential test, interface patch test, zero moment rule.

1 AN EXAMPLE

To motivate the theme of the article, we study the benchmark example defined in Figure 1. A homogeneous rectangular plate in plane stress, of width $2a$ and uniform thickness, occupying domain Ω, is under uniform inplane surface tractions $+q$ on the horizontal faces. The exact stress solution is $\sigma_{yy} = q$, others zero.

Cut the plate in two halves along Γ_{12} as depicted in Figure 1(b). This divides Ω into two partitions: Ω^1 and Ω^2 (A *partition* is a *spatial* subdivision of a continuum or discrete system [1].) Partitions Ω^1 and Ω^2 are discretized into four-node bilinear quadrilateral elements as shown in Figure 1(c). Partition 1 is divided into five

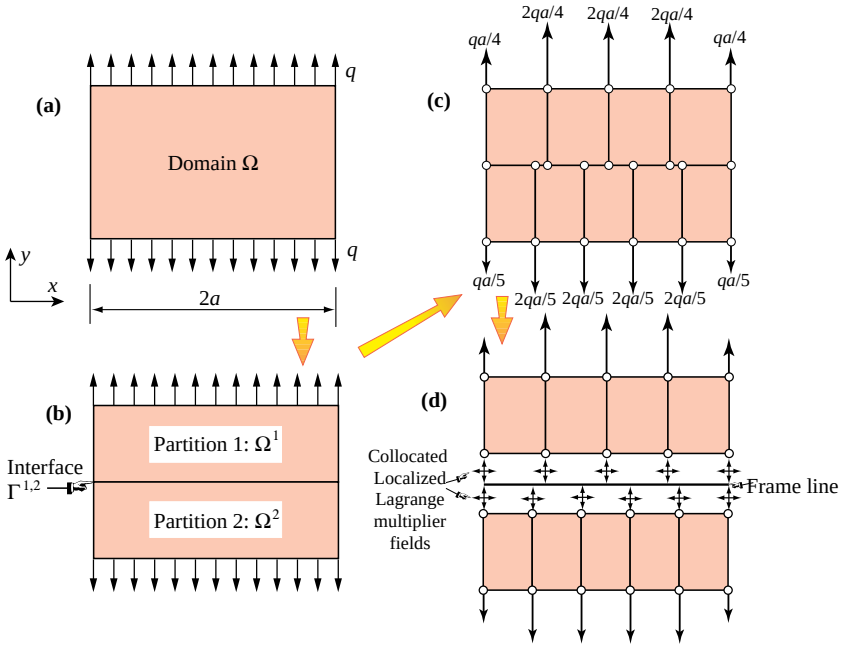

Figure 1. A benchmark problem for nonmatching FEM meshes: five bilinear elements (bottom) connected to four bilinear elements (top).

elements of equal size, and partition 2 into four. The surface traction q is converted to nodal forces by energy-consistent methods, which for these elements gives the same result as simple static load lumping.

1.1 The Interface-Mesh Connection

The theme of this article is: how can the two meshes be connected so that the constant stress solution of Figure 1(a) is exactly preserved? In answering this question one faces many choices, which may be collectively grouped into *primal* and *dual* methods. Primal methods link directly interface node displacements through some kind of master-slave interpolation scheme. These schemes have the advantage of not introducing additional unknowns, but generally violate consistency. In fact recovered stresses can be arbitrarily bad. Dual methods rely on the injection of dual variables, which in mechanical problems are the interaction forces conjugate to the interface displacements. Mathematically the interaction forces are Lagrange multipliers, hence the alternative name *multiplier methods*.

Of the set of available multiplier methods we chose, for reasons elucidated in [2–4], a *connection frame* method. A frame line is interposed between the two meshes as illustrated in Figure 1(d). The frame is endowed with a 2D displacement field $\mathbf{u}_g$, which (in the variational sense discussed later) is viewed as a primary field independent of the partition interface displacements $\mathbf{u}^1$ and $\mathbf{u}^2$. (The g subscript stands for "global," a term arising from domain decomposition applications [3].)

The frame is "glued" to each interface side through two Lagrange multiplier fields $\boldsymbol{\lambda}^1_\ell$ and $\boldsymbol{\lambda}^2_\ell$, which in a 2D problem such as this one must include normal and tangential components. The ℓ subscript stands for "localized", since each field is associated with one and only one partition.

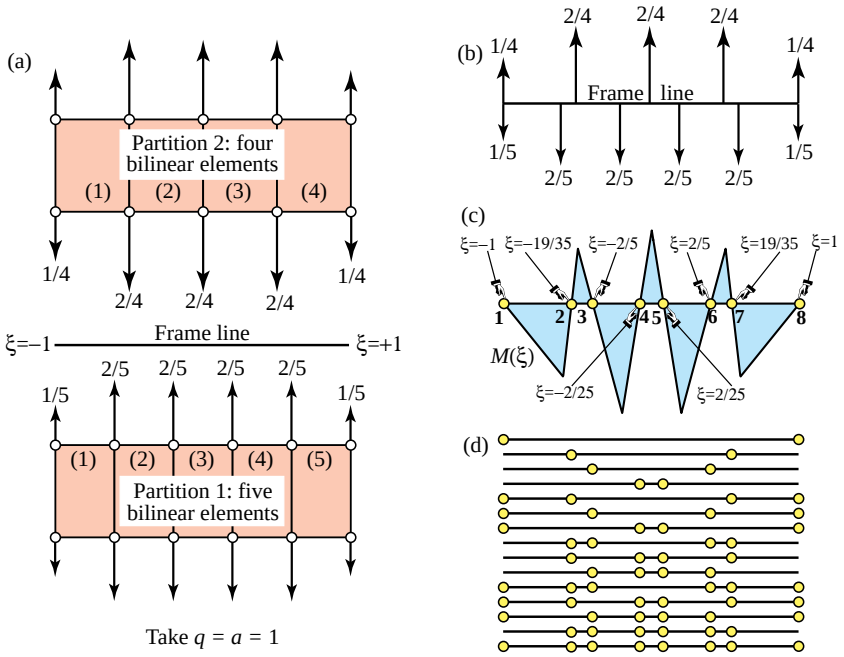

Figure 2. Placing connection frame nodes for the benchmark problem of Figure 1 by the ZMR: (a) meshes; (b) frame-FBD forces; (c) moment diagram along frame; (d) 15 symmetric frame node configurations.

Terminology for this class of mesh connection methods is yet not standardized. In the applied mathematics literature the approach is said to pertain to the class of "3-field methods", because three interface fields can vary: the partitioned domain displacement $(\mathbf{u}^1, \mathbf{u}^2)$, the frame displacement $\mathbf{u}_g$, and the Lagrange multipliers $(\boldsymbol{\lambda}^1_\ell, \boldsymbol{\lambda}^2_\ell)$. In the engineering literature one finds the terms *connector* and *interface frame*, which can be traced back to the development of hybrid elements in the late 1960s [2].

1.2 Connector Discretization Decisions

Whatever name is chosen, the three interface fields must be discretized. This leads to the following decisions:

Frame discretization. Select location of frame nodes, pick degrees of freedom (DOF) therein, and interpolate the frame displacements $\mathbf{u}_g$.

Multiplier discretization. Make similar choices for the multipliers λ^m_ℓ for $m = 1, 2$.

The decision on multiplier discretization is made first. We pick them as *concentrated forces located at partition interface nodes*, in one-to-one correspondence with the interface DOFs found there. (Mathematically, the multiplier space is that of delta functions collocated at those nodes.) This choice is computationally convenient because it avoids boundary integrals, and leads to modular mesh-coupling software, since the "coupler" needs to know little about what interface DOFs it couples with.

But it "passes the buck" to the other decision. In particular: how many frame nodes and where? If this is directly attacked from the standpoint of constant-stress consistency, and a general frame displacement interpolation assumed, we end up

with a system of generally nonlinear equations under inequality constraints on the frame node locations. Consequently, there is no *a priori* guarantee that such system will have feasible solutions.

1.3 The Zero Moment Rule

Fortunately a simple and effective rule can be invoked if the frame displacement interpolation (both normal and tangential) is *piecewise linear*. Transfer the applied nodal forces of Figure 1(c) onto the frame as illustrate in Figure 2(a), in which we have taken $a = q = 1$ to make the calculations dimensionless. Consider the frame line as an *isolated object* subject to this system of forces, and draw the free-body diagram (FBD) shown in Figure 2(b).

Frame points are located by an isoparametric-style dimensionless coordinate ξ, which varies from $\xi = -1$ at the left to $\xi = +1$ at the right. The 11 normal point forces acting on the frame FBD of Figure 2(b) are called f_i^m and act at ξ_i^m, where $i = 1, \ldots 6$ for partition $m = 1$, and $i = 1, \ldots 5$ for partition $m = 2$. Define the moment function $M(\xi)$ for $-1 \le \xi \le 1$ as

$$M(\xi) = \sum_i f_i^m \, \mathcal{R}(\xi - \xi_i^m), \quad \text{where} \quad \mathcal{R}(x-a) \stackrel{\text{def}}{=} \begin{cases} 0 & \text{if } x < a \\ x - a & \text{if } x \ge a. \end{cases} \tag{1}$$

where $\mathcal{R}(x-a)$ is McAuley's ramp function, often denoted as $\langle x-a \rangle^1$ in Mechanics of Materials textbooks. The diagram of $M(\xi)$ for the benchmark problem is shown in Figure 2(c). The Zero Moment Rule (ZMR) states that for preservation of constant-stress states

$$\boxed{\textit{Frame node locations must be located at the roots of } M(\xi) = 0.} \tag{2}$$

In the benchmark problem $M(\xi) = 0$ has eight roots at $\xi = \pm 1$, $\pm 19/35$, $\pm 2/25$ and $\pm 2/5$. (The two end nodes are of course solutions, since $M(-1) = M(1) = 0$.) The ZMR does not say *how many* frame nodes one should take. Fifteen symmetric arrangements are shown in Figure 2(d), using 2 through 8 nodes. The best configuration out of these possibilities is dictated by stability (rank sufficiency) and accuracy considerations, which are not discussed here. The rule has been verified through actual FEM calculations in contact problems [5]. An alternative procedure for the determination of frame nodal points based on the self-equilibrium conditions of the frame is presented in [6] for elasticity computations. That procedure stipulates that no additional deformation energy is created on the partitioned domains in constant stress states when they are assembled together.

Thus the rule is *necessary* but not *sufficient*. However, it reduces significantly the complexity of the original problem. Searching among a discrete set of feasible configurations, as in Figure 2(d), is an order of magnitude less taxing than starting with unknown node locations.

Structural engineers will note that $M(\xi)$ has the same interpretation as that of a *bending moment diagram* if the frame is regarded as a free-free beam. It is well known that in beam design the best places to place hinges are zero moment points. Hence engineers with that training may want to mentally convert the problem of placing frame nodes to that of selecting beam hinge locations.

2 CONNECTING ELEMENTS OF DIFFERENT ORDER

Before justifying the ZMR mathematically, it should be noted that its scope is not restricted to connecting bilinear quadrilaterals. In fact it is valid for 2D elements of varying interpolation order on either side of a straight and open interface, as long as they possess only translational freedoms, and the frame motion is interpolated by piecewise linear displacements.

To visualize the ZMR for higher order elements it is convenient to proceed graphically, drawing "interface bending moment diagrams." As noted above, this is particularly helpful for structural engineers, who are taught to draw such diagrams since undergraduate courses. If the meshes on both sides are regularly spaced with the same element type, moment functions can be compactly written for numerical experiments. For example, using *Mathematica*, functions for an interface that looks like that of Figure 1 and contains `ne` elements of identical size can be defined as

```
Ramp[xi_,a_]:= If [N[xi]>N[a],N[xi-a],0,0];
Mlin[xi_,ne_]:=Sum[(2/ne)*Ramp[xi,2*(i-1)/ne-1],{i,2,ne}]+
                   (1/ne)*Ramp[xi,-1]+(1/ne)*Ramp[xi,1];

Mqua[xi_,ne_]:=Sum[4/(3*ne)*Ramp[xi,2*(i-1)/ne-(1-1/ne)],{i,1,ne}]+
               Sum[2/(3*ne)*Ramp[xi,2*i/ne-1],{i,1,ne-1}]+
                   1/(3*ne)*Ramp[xi,-1]+1/(3*ne)*Ramp[xi,1];

Mcub[xi_,ne_]:=Sum[3/(4*ne)*Ramp[xi,2*(i-1)/ne-(1-(2/3)/ne)]+
               3/(4*ne)*Ramp[xi,2*(i-1)/ne-(1-(4/3)/ne)],{i,1,ne}]+
               Sum[2/(4*ne)*Ramp[xi,2*i/ne-1],{i,1,ne-1}]+
               1/(4*ne)*Ramp[xi,-1]+1/(4*ne)*Ramp[xi,1];
```

These functions assume that boundary forces are scaled such that they add up to 2 on each interface side. Functions `Mlin`, `Mqua` and `Mcub` pertain to 2D elements with boundary displacements varying linearly, quadratically and cubically, respectively. With these functions in place one can solve what on first look appear to be intractable mesh-connection problems in a few seconds. For example, the plot of Figure 2(c) was produced by saying

`Plot[Mlin[xi,5]-Mqua[xi,2],{xi,-1,1}, AxesOrigin->{0,0}]`.

2.1 Example 2: Linear-Quadratic Nonmatching Meshes

The second example considers again the original problem of Figure 1(a) with $a = q = 1$. The bottom partition is again discretized by five bilinear quadrilaterals but the top partition consists of two biquadratic 9-node quadrilaterals as depicted in Figure 3(a). Coordinate ξ is defined as before. Consistent node forces are shown in Figure 3(a) and mapped on the frame-FBD as depicted in Figure 3(b). A plot of the moment function $M(\xi)$ is generated by the *Mathematica* command

`Plot[Mlin[xi,5]-Mqua[xi,2],{xi,-1,1}, AxesOrigin->{0,0}]`.

The resulting moment diagram is shown in Figure 3(c). It has six zero roots at $\xi = \pm 1$, $\pm 9/35$ and $\pm 3/25$, which are candidates for frame node locations. Figure 3(d) shows 7 possible symmetric frame node configurations. The selection from these seven is done according to other criteria not discussed here.

It is important to note that this solution is not restricted to matching bilinear and biquadratic elements. The same frame forces would be produced, for instance, if each bilinear quadrilateral is replaced by two linear 3-node triangles, and each biquadratic quadrilateral by two quadratic 6-node triangles. Further, the internal

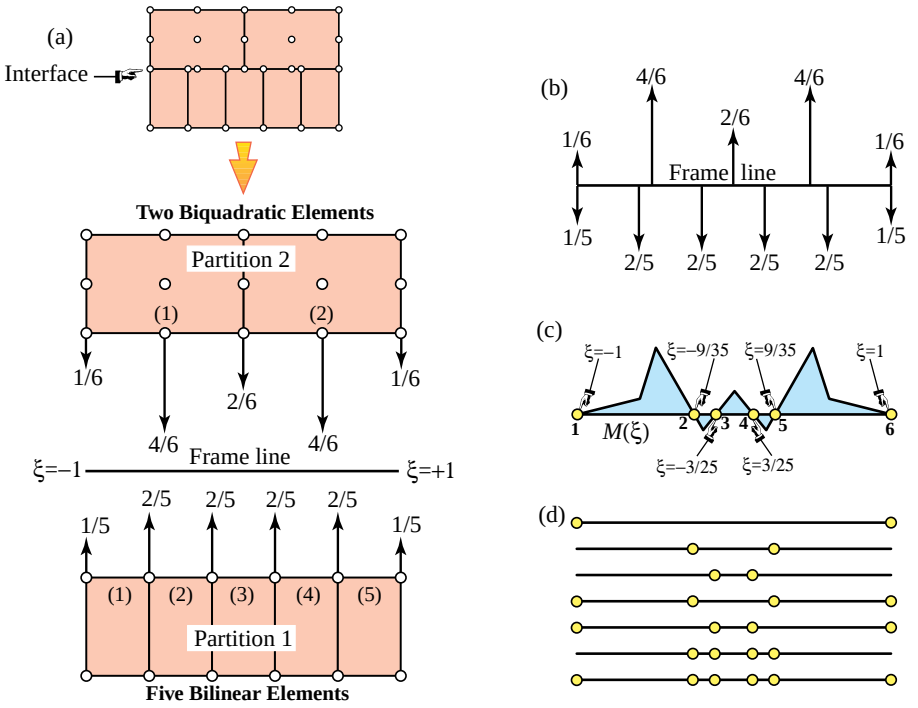

Figure 3. Five bilinear elements (bottom) connected to two biquadratic elements (top): (a) meshes; (b) frame-FBD forces; (c) moment diagram; (d) 12 symmetric frame node configurations.

element formulation: displacement, hybrid, etc., is irrelevant. This is important as regards maintaining *software modularity* should meshes to be linked be extracted from commercial FEM programs.

2.2 Example 3: Quadratic-Cubic Nonmatching Meshes

This example aims at illustrating a rather special case in which both *nodes and freedoms match at the interface*, but the displacement boundary variation does not. Again consider the problem of Figure 1(a) with $a = q = 1$. The bottom partition is discretized into three biquadratic 9-node quadrilaterals and the top one into two bicubic 16-node elements, as depicted in Figure 4(a). Coordinate ξ is defined as before. Consistent node forces are shown in Figure 4(a) and mapped on the frame-FBD as shown in Figure 4(b). A plot of the moment function $M(\xi)$ is generated by the *Mathematica* command

```
Plot[Mqua[xi,3]-Mcub[xi,2],{xi,-1,1}, AxesOrigin->{0,0}].
```

The resulting moment diagram is shown in Figure 4(c). It has six zero roots at $\xi = \pm 1$, $\pm 7/12$ and $\pm 4/21$, which are candidates for frame node locations. Figure 4(d) shows 7 possible symmetric frame node configurations. Note that *interior frame node locations do not match the partition nodes locations*. Hence it would be an error to connect the meshes as if the nodes and freedom matched.

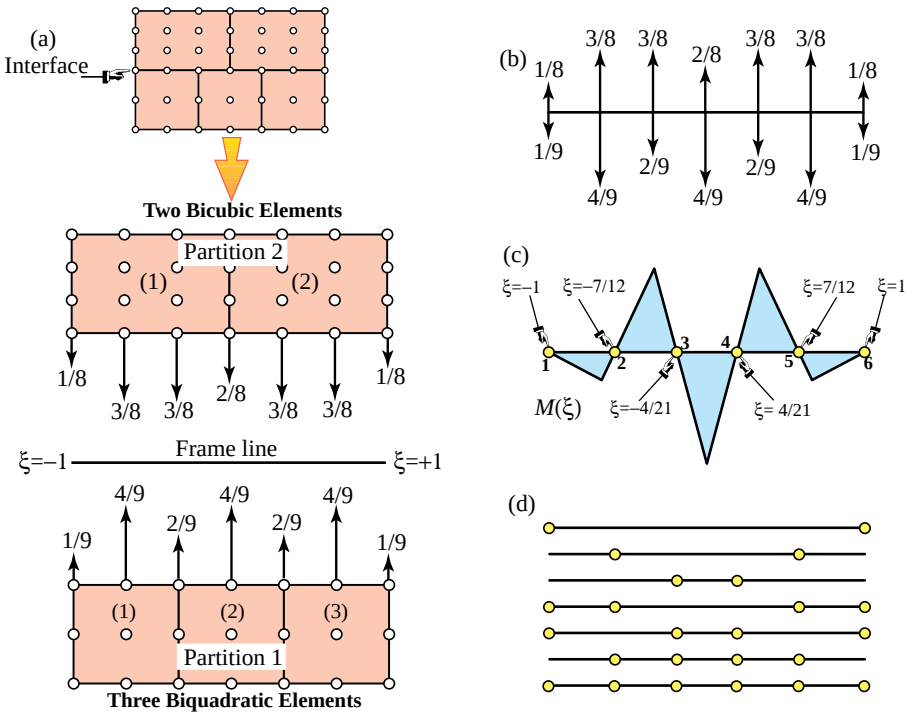

Figure 4. Three quadratic elements (bottom) connected to two bicubic elements (top): (a) meshes; (b) frame-FBD forces; (c) moment diagram; (d) 7 symmetric frame node configurations.

3 JUSTIFYING THE ZMR FROM THE IPT

The ZMR can be proven, or at least justified, in a surprising variety of ways, which range from pure variational mathematics (such as that given in the Appendix) through heuristic arguments. Proofs may rely on finite element concepts or be dissociated from them; independence being useful for extension to other discretizations such as BEM or FDM. The argument that follows is algebraic-variational in nature, and uses FEM tools such as shape functions. (Readers uninterested in these gyrations should skip directly to the Summary section).

3.1 Variational Formulation

To keep unessential clutter to a minimum, only a slight generalization of the problem of Figure 1 is considered. A free-free plate is subjected to a force system consistent with the constant plane stress solution $\sigma_{yy} = q$, others zero. We take two plate partitions: 1 and 2, discretized into nonmatching FEM meshes, as illustrated in Figure 5(a).

The following geometric and discretization restrictions are enforced: (1) the interface $\Gamma^{1,2}$ is a straight open line fully covered by elements from both sides, (2) the elements have only translational freedoms, (3) the multipliers are collocated on partition boundary nodes. Frame points are located by coordinate x. The two generalizations from the three example problems is that element sizes are arbitrary, and the frame displacements are not required to be piecewise linear.

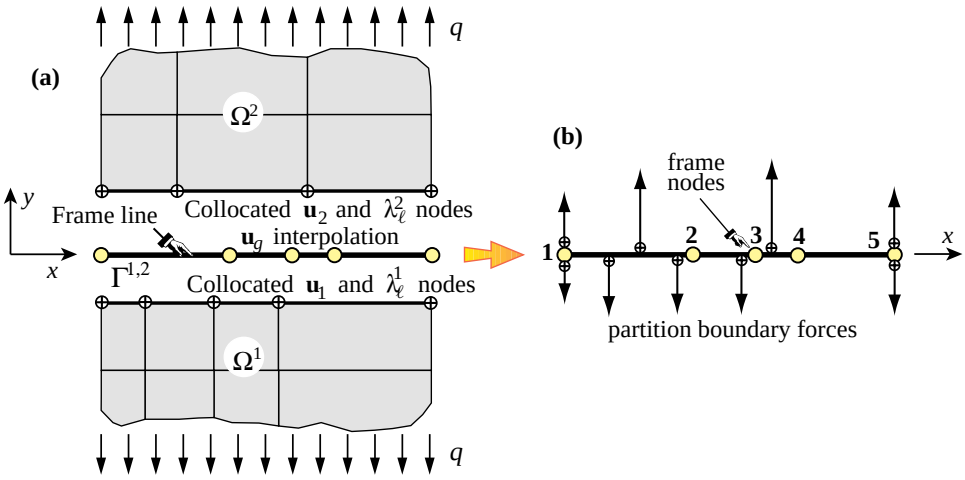

Figure 5. Connecting two nonmatched plane stress meshes to explain the IPT. (a) connection schematics: crossed partition boundary nodes are a reminder that two Lagrange multiplier freedoms "live" there; (b) connection frame as free-free object endowed with partition boundary freedoms and forces.

The problem will be further reduced in the next subsection by assuming that mesh elements are rank sufficient and satisfy the constant stress consistency condition (*sotto voce*, the patch test). All freedoms not pertaining to the interface will be statically condensed out, and the problem reduced to that depicted in Figure 5(b). This is called the *frame-reduced system*, in which the frame is viewed as a free-free object with "attached" partition nodes, and gets rid of partition fabrication details. Partition boundary nodes are marked with a cross as a reminder that two Lagrange multiplier freedoms "live" on each side.

The discrete governing functional for a quasistatic case is given by

$$\Pi(\mathbf{u}^1,\boldsymbol{\lambda}^1_\ell,\mathbf{u}^2,\boldsymbol{\lambda}^2_\ell,\mathbf{u}_g) = \Pi^1(\mathbf{u}^1,\boldsymbol{\lambda}^1_\ell) + \Pi^2(\mathbf{u}^2,\boldsymbol{\lambda}^2_\ell) + \pi^{1,2}(\boldsymbol{\lambda}^1_\ell,\boldsymbol{\lambda}^2_\ell,\mathbf{u}_g). \tag{3}$$

Here Π^m is the functionals for the separated partitions $m = 1, 2$, and $\pi^{1,2}$ is the *frame potential* that "glues" Π^1 and Π^2. In this form $\mathbf{u}^m$, $\boldsymbol{\lambda}^m_\ell$ $(m = 1, 2)$ and $\mathbf{u}_g$ denote nodal values. The continuum version of (3) is discussed in [2].

For further use we split $\mathbf{u}^m$ into interface freedoms $\mathbf{u}^m_b$ (at the crossmarked nodes of Figure 5) and the remainder: $\mathbf{u}^m_i$. The FEM equations are obtained from the first-variation stationarity condition $\delta\Pi = 0$, which gives [2]

$$\delta\Pi = \begin{bmatrix} \delta\mathbf{u}^1_i \\ \delta\mathbf{u}^1_b \\ \delta\boldsymbol{\lambda}^1 \\ \delta\mathbf{u}^2_i \\ \delta\mathbf{u}^2_b \\ \delta\boldsymbol{\lambda}^2 \\ \delta\mathbf{u}_g \end{bmatrix}^T \left(\begin{bmatrix} \mathbf{K}^1_{ii} & \mathbf{K}^1_{ib} & \mathbf{0} & \mathbf{0} & \mathbf{0} & \mathbf{0} & \mathbf{0} \\ \mathbf{K}^1_{bi} & \mathbf{K}^1_{bb} & -\mathbf{I}^1 & \mathbf{0} & \mathbf{0} & \mathbf{0} & \mathbf{0} \\ \mathbf{0} & -\mathbf{I}^1 & \mathbf{0} & \mathbf{0} & \mathbf{0} & \mathbf{0} & \mathbf{C}^1 \\ \mathbf{0} & \mathbf{0} & \mathbf{0} & \mathbf{K}^2_{ii} & \mathbf{K}^2_{ib} & \mathbf{0} & \mathbf{0} \\ \mathbf{0} & \mathbf{0} & \mathbf{0} & \mathbf{K}^2_{bi} & \mathbf{K}^2_{bb} & -\mathbf{I}^2 & \mathbf{0} \\ \mathbf{0} & \mathbf{0} & \mathbf{0} & \mathbf{0} & -\mathbf{I}^2 & \mathbf{0} & \mathbf{C}^2 \\ \mathbf{0} & \mathbf{0} & (\mathbf{C}^1)^T & \mathbf{0} & \mathbf{0} & (\mathbf{C}^2)^T & \mathbf{0} \end{bmatrix} \begin{bmatrix} \mathbf{u}^1_i \\ \mathbf{u}^1_b \\ \boldsymbol{\lambda}^1 \\ \mathbf{u}^2_i \\ \mathbf{u}^2_b \\ \boldsymbol{\lambda}^2 \\ \mathbf{u}_g \end{bmatrix} - \begin{bmatrix} \mathbf{f}^1_i \\ \mathbf{0} \\ \mathbf{0} \\ \mathbf{f}^2_i \\ \mathbf{0} \\ \mathbf{0} \\ \mathbf{0} \end{bmatrix} \right) = 0. \tag{4}$$

Here the $\mathbf{K}^m$'s and $\mathbf{f}^m$'s are the stiffness matrices and applied force vectors, respectively, for partition Ω^m; $\mathbf{I}^m$ are identity matrices of appropriate order;

and $\mathbf{C}^m$ are *connection matrices* that link the frame to partition m. The $\mathbf{C}^m$ matrices are constructed by evaluating frame displacements on the mesh nodes. Condensation of the $\mathbf{u}_i^m$ (interior) freedoms gives the frame-reduced system

$$\delta\Pi = \begin{bmatrix} \delta\mathbf{u}^1 \\ \delta\boldsymbol{\lambda}^1 \\ \delta\mathbf{u}^2 \\ \delta\boldsymbol{\lambda}^2 \\ \delta\mathbf{u}_g \end{bmatrix}^T \left(\begin{bmatrix} \mathbf{K}_b^1 & -\mathbf{I}^1 & \mathbf{0} & \mathbf{0} & \mathbf{0} \\ -\mathbf{I}^1 & \mathbf{0} & \mathbf{0} & \mathbf{0} & \mathbf{C}^1 \\ \mathbf{0} & \mathbf{0} & \mathbf{K}_b^2 & -\mathbf{I}^2 & \mathbf{0} \\ \mathbf{0} & \mathbf{0} & -\mathbf{I}^2 & \mathbf{0} & \mathbf{C}^2 \\ \mathbf{0} & (\mathbf{C}^1)^T & \mathbf{0} & (\mathbf{C}^2)^T & \mathbf{0} \end{bmatrix} \begin{bmatrix} \mathbf{u}_b^1 \\ \boldsymbol{\lambda}^1 \\ \mathbf{u}_b^2 \\ \boldsymbol{\lambda}^2 \\ \mathbf{u}_g \end{bmatrix} - \begin{bmatrix} \mathbf{f}_b^1 \\ \mathbf{0} \\ \mathbf{f}_b^2 \\ \mathbf{0} \\ \mathbf{0} \end{bmatrix} \right) \tag{5}$$

where $\mathbf{K}_b^m = \mathbf{K}_{bb}^m - \mathbf{K}_{bi}^m(\mathbf{K}_{ii}^m)^{-1}\mathbf{K}_{ib}^m$, and $\mathbf{f}_b^m = -\mathbf{K}_{bi}^m(\mathbf{K}_{ii}^m)^{-1}\mathbf{f}_i^m$.

3.3 The Interface Potential Test

Equations (4) are valid for any force system. Now assume that both partitions $m = 1, 2$ are in the same constant-stress state induced through force system $\mathbf{f}_b^m$ in (5). The associated displacements $\mathbf{u}_b^m$ are unique except for possibly a rigid body motion that produces no forces. The first four matrix equations in (5) are identically verified by the solution

$$\mathbf{u}_b^m = \mathbf{C}^m\mathbf{u}_g, \qquad \boldsymbol{\lambda}^m = \mathbf{f}_b^m - \mathbf{K}_b^m\mathbf{u}_b^m = \mathbf{f}_b^m - \mathbf{K}_b^m\mathbf{C}^m\mathbf{u}_g, \tag{6}$$

Observe that if $\mathbf{f}_b^m$ produces a constant stress state, then the interface forces, $\boldsymbol{\lambda}^m$, acting on the frame must also preserve the corresponding constant stress state. Thus, the meaning of $\mathbf{u}_b^m = \mathbf{C}^m\mathbf{u}_g$ is: the constant-stress solution displacement must be reproduced exactly (pointwise) by the frame displacements. Variation of $\pi^{1,2}$ with respect to the frame displacement $\mathbf{u}_g$ leads to

$$\delta\pi_g^{1,2} \stackrel{\text{def}}{=} \delta\mathbf{u}_g^T\left[(\mathbf{C}^1)^T\boldsymbol{\lambda}^1 + (\mathbf{C}^2)^T\boldsymbol{\lambda}^2\right] = 0 \tag{7}$$

Note that (7) mus be verified for *all variations* $\delta\mathbf{u}_g$ that are *kinematically admissible* with respect to the assumptions made on frame displacements, namely degrees of freedom and interpolation. Despite its apparent simplicity, (7) may in fact be a highly complex expression because $\delta\mathbf{u}_b$, $\mathbf{C}_1$ and $\mathbf{C}_2$ are functions of the number of frame nodes and their location, which is exactly the problem we are trying to solve. We can now state the Interface Potential Test or IPT as

> The variation (7) of the interface potential must vanish identically for all kinematically admissible frame motions while under constant-stress interface forces $\boldsymbol{\lambda}^1$ and $\boldsymbol{\lambda}^2$.

Physically this says that no spurious energy can be absorbed or released by the frame when the adjacent meshes are in a uniform stress state. Note that the IPT involves only the motion of the frame, viewed as a free-body object, under the known interface forces. A glance at (7) shows that the variation has the same form as the Principle of Virtual Work (PVW) *if the frame node locations are regarded as given*. So a technically equivalent statement, possibly more easily grasped by an engineer familiar with the PVW, is

> The virtual work $\delta\pi^{1,2}$ of the frame on the constant-stress interface forces $\boldsymbol{\lambda}^1$ and $\boldsymbol{\lambda}^2$ must vanish for all kinematically admissible virtual frame displacements, $\mathbf{u}_g$.

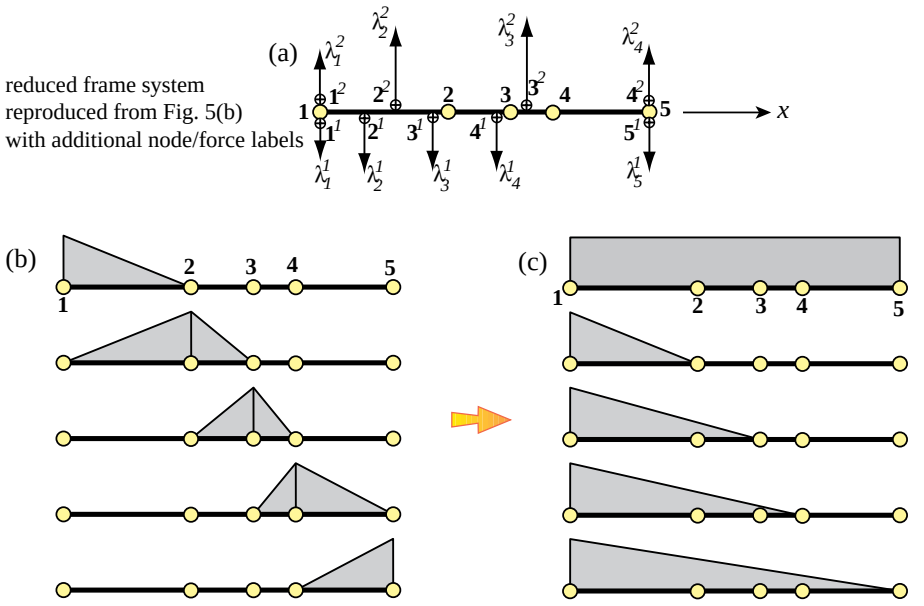

Figure 6. Example illustrating equivalence of IPT and the zero moment condition (10) for the frame of Figure 5 under piecewise-linear displacements: (a) frame discretized into four elements; (b) frame patch functions; (c) rigid body motions about nodes as "hinges".

The complexity of the frame location problem comes from two sources. If the frame interpolation is nonlinear in the frame coordinate x, $\delta\mathbf{u}_g$ is also nonlinear in x. Furthermore entries of the connection matrices $\mathbf{C}^1$ and $\mathbf{C}^2$ are discontinuous at partition node locations. So the innocent looking system (7) in fact leads to a system of nonlinear equations with inequality constraints. As noted before there is no guarantee that this system will have real solutions, and that those real solutions will be within the interface segment. A substantial simplification occurs, however, if the frame displacements is piecewise linear, which leads directly to the ZMR.

3.4 Equivalence of IPT and ZMR for Piecewise Linear Frame

The reduced frame system of Figure 5(b) is reproduced in Figure 6(a) with additional node and force labels required for the manipulations that follow. To derive the ZMR we assume that frame displacements are *piecewise linear* in both normal and tangential directions. For simplicity, however, only normal-to-the-frame displacements and forces are treated. The frame is pictured as discretized with five nodes and four frame elements (although two nodes are placed at the frame ends, this is not strictly necessary.) The frame nodes are $1, \ldots, 5$. The frame-attached boundary nodes from partition m are labeled $1^m, 2^m, \ldots$. Symbol λ_n^m labels the normal-to-the-frame constant-stress force at node n of partition m.

As this point we introduce some FEM paraphernalia and do a hat trick. The five normal-displacement patch trial functions (the well known "hat" functions) associated with the frame nodes are shown in Figure 6(b). Although in principle these could be used for the IPT (7), they provide little insight. Consider instead the five frame motions depicted in Figure 6(c). The top one is a normal rigid-body translation. The bottom four depict rigid body rotations about four frame nodes:

2, 3, 4 and 5, viewed as *hinges*; that is, only the left portion of the frame moves. (Considering node 1 as hinge gives of course nothing). It is easily verified that the five motions can be built as unique linear combinations of the hat functions of Figure 9(b), since the transformation matrix, not shown here, is triangular and square nonsingular. Hence the IPT can be indistinctly applied to either set.

Passing the IPT for the normal rigid-body translation requires that the sum of the normal forces acting on the *entire frame* vanish. This is automatically satisfied if constant stress states are correctly lumped to boundary nodes, and places no constraints on frame node location. The situation changes when the rotational motions are considered. For the sake of specificity take the rotation about hinge-node 3 located at $x = x_3$. Examination of the figure shows that five constant-stress partition-boundary forces: λ_1^1, λ_2^1, λ_3^1, λ_4^1, λ_1^2 and λ_2^2 work on the lateral displacements, which are $\alpha(x_3 - x_1^1)$, $\alpha(x_3 - x_2^1)$, etc., with α as rotational rigid motion amplitude. Then the IPT, in PVW disguise, is

$$\begin{aligned}\delta W_3 = \delta\alpha\, \big[\lambda_1^1(x_3{-}x_1^1) + \lambda_2^1(x_3{-}x_2^1) + \lambda_3^1(x_3{-}x_3^1) + \lambda_4^1(x_3{-}x_4^1) + \lambda_1^2(x_3{-}x_1^2){+}\\ {+}\lambda_2^2(x_3{-}x_2^2)\big] = \delta\alpha\, M_3 = 0, \qquad \text{whence} \quad \boxed{M_3 = 0}\end{aligned} \tag{8}$$

If the "hinge position" is generically denoted by x, M_3 generalizes to the moment function

$$M(x) = \sum_{i,m} \lambda_i^m\, \mathcal{R}(x - x_i^m), \quad \text{where} \quad \mathcal{R}(x-a) = \begin{cases} 0 & \text{if } x < a \\ x - a & \text{if } x \ge a. \end{cases} \tag{9}$$

in which $m = 1, 2$ and i runs over all forces from subdomain m, with appropriate signs. But this is precisely the ZMR stated, as recipe, in Section 1.3.

As regards shearing boundary forces and tangential frame displacements, the same argument applies without changes. The frame locations must be at the roots of $M(x) = 0$. The difference is that tangential frame motions cannot be physically interpreted as rigid rotations about hinges, and *the IPT is no longer an equilibrium condition*. In summary: the ZMR suffices for frame node placement with respect to *all* piecewise-linear motions, whether normal or tangential.

4 SUMMARY: HOW EXTENDIBLE IS ZMR?

The rule is so simple that one is tempted to see whether it extends to more complicated situations. Here are additional scenarios listed roughly in order of increasing complexity:

(a) Constant shear consistency tests and tangential displacements
(b) Curved 2D interfaces
(c) Partial 2D interfaces
(d) Rotational degrees of freedom
(e) General 2D interfaces with multiple branches and closed circuits
(f) 3D interfaces
(g) Contact and sliding
(h) Higher order frame interpolation
(i) Dynamic response problems
(j) Different discretizations, e.g., FEM/BEM or FEM/FDM

(k) Multiphysics interfaces

The ZMR extends with only minor changes to scenarios (a,b,c); in fact for (a) in 2D the answer is given in the previous subsection. Extensions to (d,e,f) are presently under study — for (f) the equivalent rule involves the Poisson equation. Modeling contact, with and without friction, is of course one of the major sources of nonmatching meshes, and recent studies [5] have shown that the ZMR works effectively in 2D if used in an iterative setting. The ZMR breaks down under scenario (h) and in fact no solution to the frame node placement problem generally exists, even in 2D. For scenarios (i,j,k) new physical interpretations are required.

For 3D nonmatching interface meshes that are rectangular with rectangular partitioned boundary domains, a simple and effective frame discretization procedure [6] is available. For arbitrary irregular interface meshes, further 'localizations' of the interface potential $\pi^{1,2}$ are necessary.

Is failure in more complicated scenarios reason for alarm as regard the universality of the interface frame approach? No. There are two safety nets:

1. Smoother interpolation spaces may be used for the localized Lagrange multiplier fields. If this is done, higher order frame interpolations become feasible. However, the formation of mesh-coupling matrices becomes more involved because field integrations over the interface boundaries are required, and the resulting software is much less modular.
2. The IPT (Interface Patch Test or Interface Potential Test, whichever the reader prefers) is generally applicable as long as the interface potential functional π can be expressed in term of frame variables — whatever they are — and localized multipliers — whatever they mean. Then $\delta\pi = 0$ over the space of admissible variations of frame primal variables is the test of last resort.

So the cautious answer is: the ZMR does have limited application range, but it covers a useful range of nonmatching mesh-connection problems. The IPT is more general, but translating it to precise rules for the practicing engineer is likely to require specialization of the problem domain.

ACKNOWLEDGEMENTS

Preparation of the present paper has been supported Lawrence Livermore National Laboratories under the Scalable Algorithms for Massively Parallel Computations ASCI L2 contract B-347880 and by the National Science Foundation under Grant ECS-9725504.

REFERENCES

[1] C. A. Felippa, K. C. Park and C. Farhat, Partitioned analysis of coupled mechanical systems, Invited Plenary Lecture, Fourth World Congress in Computational Mechanics, Buenos Aires, Argentina, July 1998, expanded version to appear in *Comp. Meths. Appl. Mech. Engrg.* Special Issue on FSI, 2001.

[2] K. C. Park and C. A. Felippa, A variational principle for the formulation of partitioned structural systems, *Int. J. Numer. Meth. Engrg.*, **47**, 395–418, 2000.

[3] K. C. Park, U. Gumaste and C. A. Felippa, A localized version of the method of Lagrange multipliers and its applications, *Comput. Mech. J.*, **24/6** 476–490, 2000.

[4] K. C. Park and C. A. Felippa, A variational framework for solution method development in structural mechanics, *J. Appl. Mech.*, **65/1**, 242–249, 1998.

[5] G. Rebel, K. C. Park and C. A. Felippa, A contact-impact formulation based on localized Lagrange multipliers, Center for Aerospace Structures, Report No. CU-CAS-00-18, University of Colorado, Boulder, CO, July 2000; submitted to *Int. J. Numer. Meth. Engrg.*.

[6] K. C. Park, C. A. Felippa and G. Rebel, A simple algorithm for localized construction of nonmatching structural interfaces, Center for Aerospace Structures, Report No. CU-CAS-00-22, University of Colorado, Boulder, CO, September 2000; submitted to *Int. J. Numer. Meth. Engrg.*.

APPENDIX - A PURELY VARIATIONAL PROOF OF THE ZMR

This proof looks at the reduced frame system, Figure 6(a), as simply a mechanical object under the given force system $q(x) = \lambda_i^m \delta(x_i^m)$ where $\delta(.)$ is the delta function. The force source: FEM nodes, BEM control points or finite difference gridpoints, is irrelevant. (In fact $q(x)$ can be anything: point forces, distributed forces such as pressures, or a mixture of the two.) The following proof relies on just one assumption: the virtual work of the frame on all admissible test functions (the virtual frame displacements) must be zero.

The interface extends from $x = 0$ through $x = L$. For the ensuing manipulations it is convenient to *extend* the frame outside the interface proper so that its end points A, B are at $x_A = -a$ and $x_B = L + b$, where a and b are arbitrary positive values. The frame nodes are located at x_n, $n = 1, \ldots N$ with $0 \le x_n \le L$. Also $x_{n+1} > x_n$, that is, no coincident nodes are allowed. Coordinates x_1 and x_N are taken as location of the first and last frame nodes, respectively, a decision subject to *a posteriori* verification. The transverse displacement of the frame is $w(x)$, which is taken to be C^0 continuous and piecewise-linear between frame nodes. This is conventionally prolonged with constant values to cover the remainder of the frame, so that $w(x) = w(x_1)$ for $x_A \le x \le x_1$, and $w(x) = w(x_N)$ for $x_N \le x \le x_B$. The test function for the PVW is δw.

Call $V = V_A + \int_A^x q(x)\,dx$ and $M(x) = M_A + \int_0^x V(x)\,dx$ so that $q = d^2M/dx^2 = M''$, where $(.)' \equiv d(.)/dx$. From those definitions $V(x)$ and $M(x)$ are the transverse shear and bending moment functions, respectively, associated with the force system $q(x)$.

The frame virtual work is $\delta W = \int_A^B q(x)\,\delta w(x)\,dx$. Setting δw to be a linear function in $x \in [0, L]$ requires the applied forces to satisfy global translational and rotational equilibrium, but places no conditions on frame node locations. To do that δW is integrated twice by parts:

$$\delta W = M_A\,\delta w'_A - M_B\,\delta w'_B + V_B\,\delta w_B - V_A\,\delta w_A + \int_A^B M(x)\,w''\,dx. \tag{10}$$

But $\delta w'_A = \delta w'_B = 0$ since $w(x)$ is constant there. Next, take $\delta w_A = \delta w_1 = 1$, $\delta w_B = \delta w_N = 0$, and interpolate linearly between w_1 and w_N; then $\delta W = V_A = 0$ because there are no forces between x_A and $x_1 = 0$. Likewise take $\delta w_A = \delta w_1 = 0$, $\delta w_B = \delta w_N = 1$, and a linear interpolation between w_1 and w_N; then $\delta W = V_B = 0$ because there are no forces between $x_N = L$ and x_B. Consequently all boundary terms in (10) vanish.

Since $w(x)$ is piecewise linear between frame nodes so is $\delta w(x)$. At a frame node n the following weighted-finite-difference relation holds:

$$\delta w''_n = \frac{\delta w_{n+1} - \delta w_n}{\Delta x_n^+} - \frac{\delta w_n - \delta w_{n-1}}{\Delta x_n^-} \tag{11}$$

where $\Delta x_n^+ = x_{n+1} - x_n > 0$ and $\Delta x_n^- = x_n - x_{n-1} > 0$. For the first node ($n = 1$), $x_{n-1} = x_0$ is conventionally taken to be at A; for the last node ($n = N$), x_{n+1} is taken to be at B. At location other than nodes, $\delta w'' = 0$. Hence

$$\delta W = \sum_n M(x_n)\delta w''(n) = \sum_n M(x_n) \left(\frac{\delta w_{n+1} - \delta w_n}{\Delta x_n^+} - \frac{\delta w_n - \delta w_{n-1}}{\Delta x_n^-} \right) = 0. \tag{12}$$

At nodes $n = 2, \ldots N-1$ take $\delta w_{n+1} = \delta w_{n-1} = 0$, $\delta w_n = 1$; since $\Delta x_n^+ > 0$ and $\Delta x_n^- > 0$, (12) requires $M(x_n) = 0$. At node 1 take $\delta w_A = \delta w_1 = 1$ and $\delta w_2 = 0$, which requires $M(x_1) = 0$. At node N take $\delta w_N = \delta w_B = 1$ and $\delta w_{N-1} = 0$, which requires $M(x_N) = 0$. Thus function $M(x)$ must vanish at all frame nodes. We note that $M(x_1) = M(x_N) = 0$ because there are no forces to the left of $x = x_1$ and to the right of $x = x_N$, thus justifying the *a priori* choice of those locations as first and last frame nodes, respectively. Consequently the ZMR is proved.